Available online at www.sciencedirect.com

ScienceDirect

Procedia Computer Science 180 (2021) 482–491

Procedia Computer Science

www.elsevier.com/locate/procedia

International Conference on Industry 4.0 and Smart Manufacturing

Simulation of ground bearing pressure profile under hydraulic crane outrigger mats for the verification of 16-point combined loading

Ghulam Muhammad Ali[a,*], Asif Mansoor[a], Shuai Liu[a], Jacek Olearczyk[a], Ahmed Bouferguene[b], Mohamed Al-Hussein[a]

[a]*Dept. of Civil and Environmental Engineering, University of Alberta, Edmonton, Alberta, Canada*
[b]*Campus Saint Jean, University of Alberta, Edmonton, Alberta, Canada*

Abstract

The modular construction approach relies heavily on mobile cranes. With the increase in weight of modules, the ground bearing pressure (GBP) applied by the hydraulic crane also increases. To avoid ground failure, the primary technique is to determine the GBP by calculating the resulting force at each outrigger and assuming it is distributed uniformly over the surface area of the mat under the outrigger. Finite element analysis (FEA) indicates that the pressure profile beneath the crane mat is not uniform in nature, which means the traditional method of calculating the GBP is inaccurate. In this study, a new method is proposed to determine the GBP profile. The proposed methodology can determine the GBP at 16 points, the four corners of each of the four outriggers. For a theoretical case study, a hydraulic crane Grove GMK 7550 with three different payloads is examined and the results are verified by using FEA.

Keywords: Hydraulic crane, ground bearing pressure, finite element analysis, combined loading

Nomenclature

COG	centre of gravity
FEA	finite element analysis
GBP	ground bearing pressure

* Corresponding author. Tel.: +1-780-492-9155.
E-mail address: gmali@ualberta.ca

1877-0509
10.1016/j.procs.2021.01.264

1. Introduction

Construction 4.0 is the term used to describe the application of Industry 4.0 approaches to construction, which point the various phases of construction toward automation and digitization. Construction 4.0 involves the development of a smart construction site, data storage, and simulation [1,2]. Simulation, in particular, allows companies to evaluate, in advance of a project, the various construction phases to determine how best to accomplish their safe and timely completion at a higher quality and at a reduced cost [1,2]. There are two main categories of construction methodology: on-site construction and off-site construction, of which modular construction is a common approach. Modular construction involves the planning, designing, fabrication, and assembly of building elements at a separate location away from the actual construction site. For example, a building is constructed in modules that are transported and then lifted and assembled on site to form the structure. The concept of offsite construction drives its roots from the paradigm of manufacturing industry. Lean manufacturing focuses on reducing the waste while improving value and creating a more client-centric product [3]. Seven wastes are outlined, which include over-production, defects, inventory, over processing, transportation, waiting, and motion. In the context of the construction industry, there is the potential to reduce the aforementioned wastes as much as possible in the modular construction approach, which is evolving to adopt Industry 4.0 practices to further centralize the whole construction process [4]. As a result, with time, the designing and fabricating of modules has become a familiar process, which leads engineers to front-load these modules with a growing number of features to reduce the amount of on-site work required. A downside of increasing the level of finishing of a module is the resulting increase in the weight of the module, which in turn necessitates the use of heavy cranes, such as hydraulic cranes. The safety and success of these lifts depend primarily on the fitness of the ground support. Of course, as the weight of the lifting system (crane + payload) has increased, the ground-bearing capacity cannot be neglected, as this can cause failure of the ground resulting in loss of life and property. Many researchers have reported ground failure as the major cause of crane accidents [5–10].

The first measure to plan a lift is to define the pressure, normally known as ground bearing pressure (GBP), that the mat under the crane outriggers can exert on the ground. Traditionally, the GBP calculation is performed by taking crane components, the center of gravity (COG) of each, and their impact on the ground in the form of GBP. Crane mats are typically used to maintain an evenly distributed GBP below the soil bearing capacity. Traditionally, to determine the GBP under a hydraulic crane mat, the calculated resultant forces at each outrigger is uniformly distributed over the surface area of the mat touching the ground. The assumption is that the GBP is uniform over the surface area of the mat [11–13]. Whereas Ali et al. [14], while conducting a study on the behavior of crane mats under hydraulic outriggers using finite element analysis (FEA), observed that the GBP is not uniform in nature. At some locations under the crane mat, the GBP value was higher as compared to the GBP values calculated using the traditional method. Assuming a uniformly distributed GBP under the crane mat can be inaccurate. As the construction industry is deploying cranes with heavier weights and higher capacities with the passage of time, neglecting these variations could result in catastrophic failures. A couple of years ago, these variations could be ignored, but with the increase in module weights and the integration of Construction 4.0 practices, where all the data can be linked, these variations can no longer be ignored at the expense of crane stability. Practitioners are moving towards zero tolerance when it comes to safety, and with the help of technology the same practitioners are trying to be increasingly efficient and competitive. In this respect, the industry, overall, aims to have better information in order to make better decisions. Neglecting this crane stability issue can have devastating consequences for the workers involved in crane operation. To prevent this problem, this study presents a new method to calculate GBP under hydraulic crane outrigger mats. Moreover, FEA simulation is used in this study for the purpose of verifying the proposed method. Simulation, as one of the most commonly applied approaches in the context of Industry 4.0, can help reduce the chances of crane failure on a construction site before the actual critical lift. A hydraulic crane with three payloads is used as the theoretical case study to verify the proposed method. The proposed method will provide practitioners with the GBP under the hydraulic crane mat at 16 points (i.e., the four corners of each of the four crane mats, one under each of the four outriggers).

2. Literature Review

Shapiro and Shapiro [11] presented in-depth details pertaining to the calculations covering all crane weights and their center of gravity (COG)s, and the derived equations for the calculation of GBP under hydraulic crane outrigger

mats. Becker [12] also formulated the equations for GBP calculations. The GBP calculations for hydraulic cranes are slightly different from those used for crawler cranes. For a crawler crane, the GBP is calculated directly under the crawler tracks [11,12]. In the case of hydraulic cranes, first the outrigger loads in the form of reaction forces under the outriggers are calculated. Later, the surface area of the outrigger mat in contact with the ground is used to calculate the GBP exerted by that outrigger [11,12]. The reaction force and the GBP under the outriggers depends on three factors γ, ϕ and β, according to Equations (1), (2), and (3):

$$\gamma = \frac{W_s + W_c}{4 w_m l_m} \tag{1}$$

$$\phi = \frac{W_s d_s sin\theta_s + W_c d_c sin\theta_c}{B_c w_m l_m} \tag{2}$$

$$\beta = \frac{W_s d_s cos\theta_s + W_c d_c cos\theta_c + (W_s + W_c) x_o}{L_c w_m l_m} \tag{3}$$

where W_c = weight of carrier; W_s = weight of superstructure; d_c = horizontal distance of COG of carrier to the crane rotational axis (positive towards front); d_s = horizontal distance of COG of superstructure to the crane rotational axis (positive towards front); x_0 = distance between centroid of outriggers and the crane rotational axis (positive towards front); L_c = distance between outriggers lengthwise (center to center); B_c = outrigger distance from center; θ_s is the angle between the superstructure COG and the X-Axis; θ_c is the angle of carrier COG; w_m is the width of mat; and l_m is the length of mat [13,15]. Fig. 1 shows these variables with respect to a hydraulic crane model. The GBP under each outrigger with the addition of a crane mat can be calculated using Equations (4), (5), (6) and (7). These approaches were utilized later by many researchers to develop the selection criteria of cranes based on crane and ground stability [13,16].

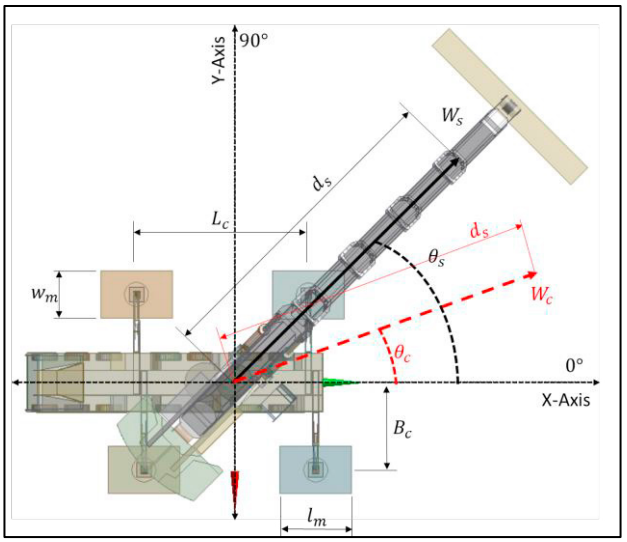

Fig. 1. Hydraulic Crane Grove GMK7550 FEA model on Cartesian coordinates system.

$$GBP_{(right\ front)} = \gamma + \frac{1}{2}(\phi - \beta) \tag{4}$$

$$GBP_{(left\ front)} = \gamma - \frac{1}{2}(\phi + \beta) \tag{5}$$

$$GBP_{(right\ rear)} = \gamma + \frac{1}{2}(\phi + \beta) \tag{6}$$

$$GBP_{(left\ rear)} = \gamma - \frac{1}{2}(\phi - \beta) \quad (7)$$

3. Methodology

3.1. Development of GBP calculation Equations

First, a set of equations for the GBP calculation under the hydraulic crane outrigger mat are developed and later these methods are verified using FEA. The GBP under the hydraulic crane mat is a typical example of combined loading [17]. As a prerequisite of combined loading, the resultant force W of all the weights of the crane parts (including payload) and the COG location of each part in the form of R and θ from X-axis need to be calculated. The combined loading is the combination of normal forces and the bending moments acting on the surface area of the crane mat, as shown in Fig. 2. The edges/corners of the crane mat are the points that will project the GBP profile under a crane mat. The mat corners for each mat outrigger can be named P1, P2, P3 & P4 for a total of 16 points (four points on each of the four outriggers).

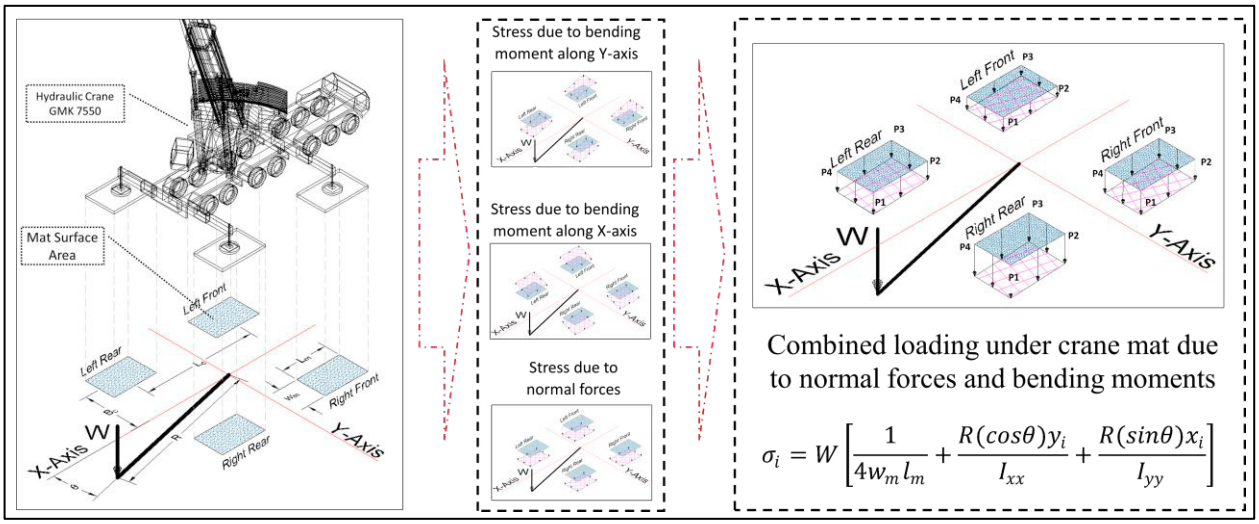

Fig. 2. Combined loading on crane mats under the hydraulic crane Grove GMK 7550.

As stated previously, the normal stress is easy to calculate as it is total weight W divided by the mat surface area $4w_m l_m$. In contrast, the bending moment due to the resultant force W depends on the location of the point where the GBP is required. For example, for the right rear outrigger, the positions of P1, P2, P3 & P4 in Cartesian coordinates are used to determine the values for bending moment along X-axis and Y-axis.

The points P1, P2, P3 & P4 for each outrigger can be described as $P_i(x_i, y_i)$, where $i = 1,2,\cdots,16$. The GBP equation can be expressed as shown in Equation (8):

$$\sigma_i = W\left[\frac{1}{4w_m l_m} + \frac{R(cos\theta)y_i}{I_{xx}} + \frac{R(sin\theta)x_i}{I_{yy}}\right] \quad (8)$$

where I_{xx} and I_{yy} are the second moments of mat surface area along X-axis and Y-axis on the Cartesian coordinates and can be calculated by Equations (9) and (10) [18]:

$$I_{xx} = \frac{1}{12}\sum_{i=1}^{n}(x_i y_{i+1} - x_{i+1} y_i)(x_{i+1}^2 + x_i^2 + x_i x_{i+1}) \quad (9)$$

$$I_{yy} = \frac{1}{12}\sum_{i=1}^{n}(x_i y_{i+1} - x_{i+1} y_i)(y_{i+1}^2 + y_i^2 + y_i y_{i+1}) \quad (10)$$

3.2. Theoretical Case Study (Grove GMK7550)

For the theoretical case study, a Grove GMK7550 hydraulic crane with a 550 ton maximum capacity is configured [19]. The details pertaining to the crane configuration used for the theoretical case study example are shown in Table 1. A picture of the crane and its FEA crane model are displayed in Fig 3. For the theoretical case study example, three different payloads, 35,000 kg, 40,000 kg, and 45,000 kg, are used. For the traditional calculations, Equations (4), (5), (6) and (7) are used to calculate the GBP under each outrigger crane mat. These equations provide a single value for each crane mat and assumes the GBP under mat is uniformly distributed based on the resultant force on the outrigger. The same crane configuration is used for the manual 16-point GBP calculation using Equation (8) to develop a GBP profile under each of the crane mats. This provides a non-uniform GBP profile under each crane mat. The values at P1, P2, P3 & P4 and the GBP (as calculated using the traditional method) under each crane mat are obtained for each 5° interval for superstructure slew from 0° to 90°, from right rear to right front.

Table 1. Hydraulic Crane Configuration (GMK7550).

Description	Detail
Boom length	38.13 m
Boom configuration	[0-100-100-0]
Superstructure counterweights	119,975 kg
Lifting radius	19.81 m
Lifting load-1	35,000 kg
Lifting load-2	40,000 kg
Lifting load-3	45,000 kg
Outrigger span	8.90 m × 8.70 m
Surface operating condition	Solid

Fig. 3. Hydraulic Crane GMK7550 with its FEA model.

To verify the accuracy of the proposed method, which uses combined loading, the same crane and mat configuration is used for FEA simulation. The model, as shown in Fig. 3, is used with ANSYS 19.2 as the FEA platform. The GBP values at P1, P2, P3 & P4 (for each outrigger mat) as determined by the FEA simulation are collected for a superstructure rotation from 0° to 90° from crane right rear to the right side at 5° intervals. For the purpose of FEA simulation and for the ease of processing, the FEA model of the GMK7550 crane is divided into three main components, the rotating part (superstructure), the stationary part (carrier or undercarriage), and crane mats. The parts are shown in Fig. 4 (a). The stationary part remains static, but the rotating part rotates to move the load from one location to another. The crane mats bear the load of the crane and transfers it to the ground.

4. Outcome and discussion

During FEA simulation, it was observed that the corners of the outrigger mat have different stress values (GBP) as compared to the GBP values calculated using the traditional method. The present study has as its objective to develop a new manual calculation method to determine the GBP variation under crane mat. For verification purposes, the FEA model of the hydraulic crane, with the same configuration and payloads, was simulated. The FEA pressure diagram under the crane mat for the payload of 35,000 kg is shown in Fig. 4 (b).

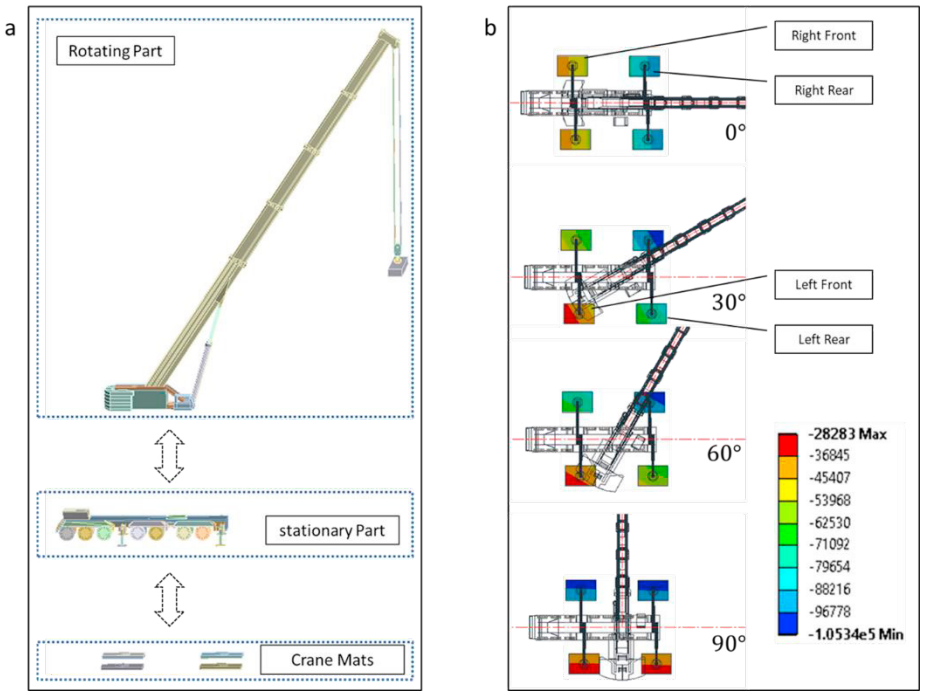

Fig. 4. (a) Hydraulic Crane GMK7550 FEA model components; (b) GBP variation under crane mat along crane superstructure slew (35,000 kg payload, values in Pa).

In Fig. 4 (b), the color variation shown on each crane mat indicates the GBP under the mat is not uniform in nature. FEA provides negative values for compressive stress. The GBP under the crane mat changes with the change in crane slew angle. The GBP value under the outrigger mat is maximum (compression) when the payload is directly over that outrigger.

It is found that the FEA GBP values at P1, P2, P3 & P4 (for each outrigger) are different from the values of GBP as calculated using the traditional method as per Equations (4), (5), (6) and (7). Moreover, the manual calculations using Equation (8) also differ from the GBP values as calculated using the traditional method. The right rear mat is shown as an example in Fig. 5 for a payload of 35,000 kg. The solid line in Fig. 5 is for GBP values as calculated using the traditional method.

Fig. 5 shows that basing ground support requirements solely on the traditional GBP calculations can lead to ground failure. For the crane mat selection, practitioners determine which outrigger mat has the maximum GBP, and consider that as the critical location for potential ground collapse. Fig. 5 shows that there is always some location on the mat where the GBP value determined using Equation (8) and using FEA is greater than the traditional GBP value. The traditional method only calculates the average over the mat, but the GBP values calculated using Equation (8) and FEA provide the upper and the lower values. Mat selection based on the traditional GBP calculations can be feasible if the GBP is uniform throughout the surface area of the mat, but not in the case where there is a variation of GBP over the surface area of the mat, with some values being greater the GBP values as calculated using the traditional

method. The follow-up question arises regarding how much variation exists between the proposed method and the traditional GBP. For that, the traditional GBP value is taken as the base line and the difference between the traditional GBP value and the values for P1, P2, P3 & P4 for each outrigger are plotted against each crane slew angle. Fig. 6 (a) (left rear outrigger mat), Fig. 6 (b) (left front outrigger mat), Fig. 7 (a) (right rear outrigger mat) and Fig. 7 (b) (right front outrigger mat) show the difference between the FEA values and the traditional GBP and also the difference between the manual calculations values using the proposed method, i.e., Equation (8), and the traditional GBP, for all three payloads (35,000 kg, 40,000 kg, and 45,000 kg).

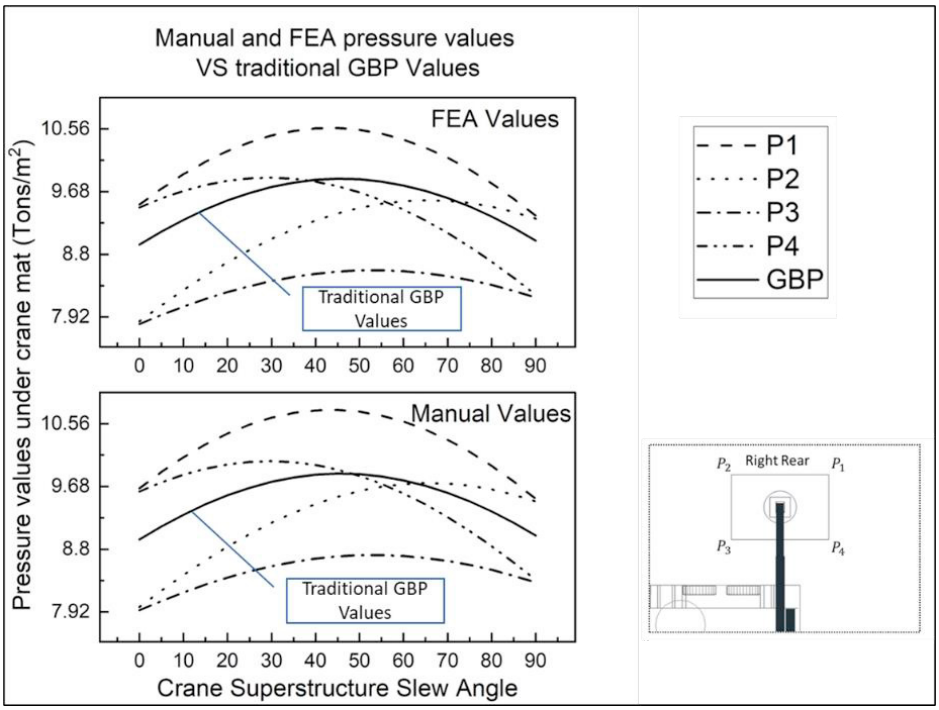

Fig. 5. GBP variation under crane mat (right rear outrigger) along crane superstructure slew (payload of 35,000 kg).

It can be observed that the difference between either the FEA or manual calculations using Equation (8) and the GBP as calculated using the traditional method is maximum for the right rear outrigger, as the payload moves from right rear to the right side of the hydraulic crane from 0° to 90°. For P1 of right rear, the GBP values from FEA and manual calculations is greater when compared to the traditional GBP. It clearly shows that the traditional calculation method is limited and the results using this traditional method can be deceiving. This implies that the chances of ground failure under a crane outrigger will increase, as will the probability for crane tipping. The values of P3 for right rear show that the actual pressure (FEA and manual) is less than GBP values as calculated using the traditional method. This creates a trapezoidal pressure under each outrigger mat. The difference is maximum (towards positive) when the payload is directly over the outrigger. With this position of the superstructure, the GBP is maximum under the mat and the far most corner of the mat experiences the maximum compression.

Considering the three theoretical case studies with three payloads, it is worthy to note that the variation increases as the payload increases. The increase in payload increases the value of W, and the value of R also increases. This implies that as the weight of the crane increases, the difference also increases between the GBP (beneath crane mat) and the GBP as calculated using the traditional method. The crane mats are used to distribute the GBP such that they do not exceed the soil bearing capacity. If the GBP value is greater, there is a greater possibility of ground failure. If the dimensions of mat were determined as per the GBP values as calculated using the traditional method, there is a likelihood that the ground may settle due to the GBP on the edges of the crane mat, specially the crane mat directly under the crane boom.

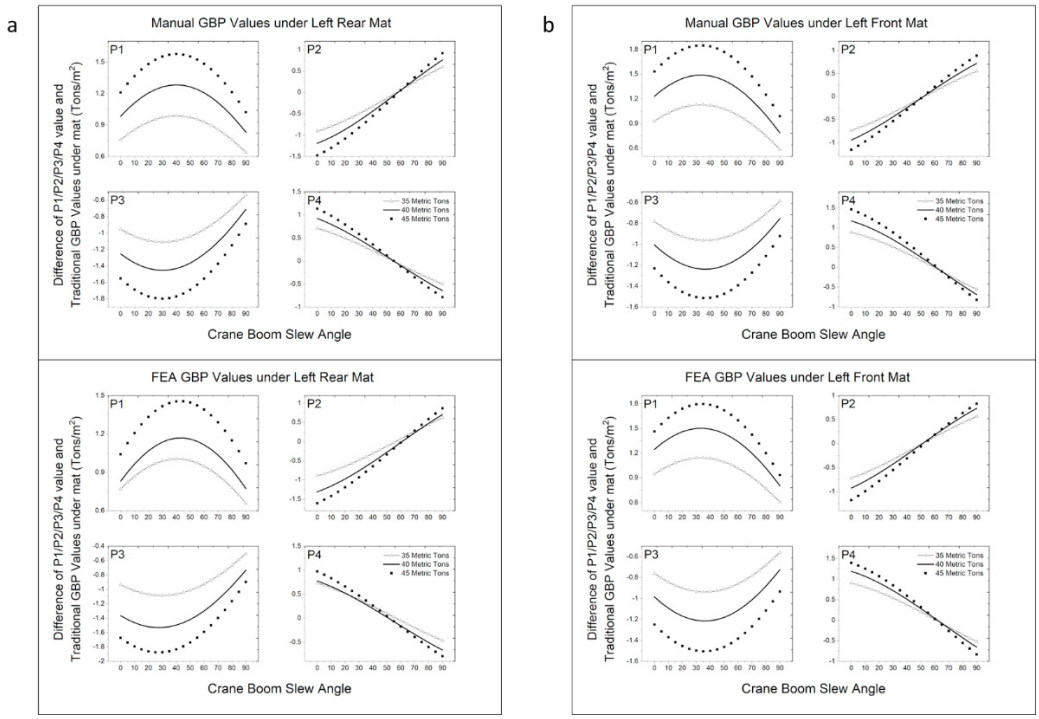

Fig. 6. Manual and FEA GBP values difference from GBP values calculated using the traditional method. (a) Left Rear Mat; (b) Left Front Mat.

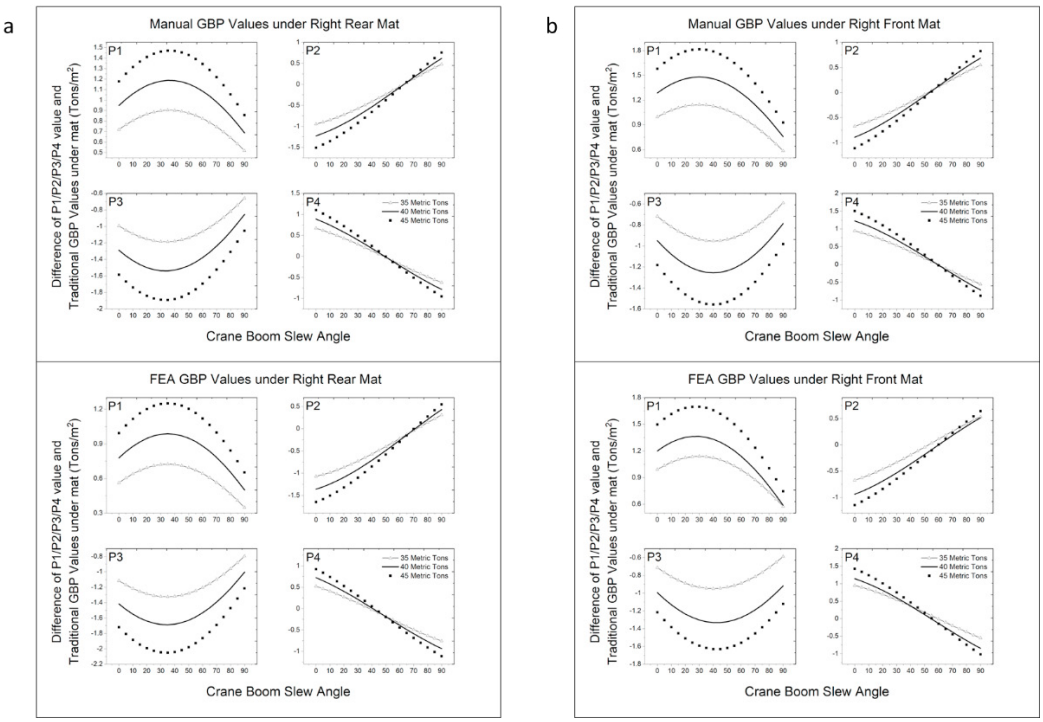

Fig. 7. Manual and FEA GBP values difference from GBP values calculated using the traditional method. (a) Right Rear Mat; (b) Right Front Mat.

As stated before, an FEA model was used for the verification of the proposed method. Fig. 6 (a & b) and Fig. 7 (a & b) show that the GBP profile generated by FEA simulation is similar to the manual calculations using Equation (8). Similarly, the right rear experiences the maximum pressure. It is noted that the average percentage difference between FEA and the proposed method, i.e., the manual calculations using Equation (8), is between 0.5% to 1%, which is negligible as compared to the GBP values as calculated using the traditional method.

The major findings of the present study are that the GBP values as calculated using the traditional method can be inaccurate and should be avoided to prevent any failure. Moreover, as the weight of the crane with payload increases, so does the magnitude of the variation of GBP under the crane mat. The present study raises a concern regarding the GBP calculations for hydraulic cranes, particularly when the construction industry is increasingly employing high capacity mobile cranes (hydraulic and crawler cranes) for module installation and assembly. It is important for practitioners to employ an additional safety factor to compensate for the actual variation in GBP. To be precise, it is vital for practitioners to calculate GBP values using Equation (8) for any critical lifts. It is worthwhile to note that from 2008 to 2015, there were 1,906 crane-related accidents in Canada alone, which is definitely a grave concern [20]. It is also worth noting that the 11% of crane accidents in the USA between 1997 and 2003 are linked with soil stability, as per Occupational Safety and Health Administration (OSHA) records [21]. The research has shown that ground failure is one of the major contributors to crane accidents that can be avoided if proper GBP/crane mat selection calculations are performed [5–8]. It is important to mention that the term Construction 4.0, which is derived from the term Industry 4.0, emphasizes the implementation of simulation and virtual reality applications to provide a more in-depth understanding of various construction phases [1,2]. In the context of the Construction 4.0 paradigm, the present study uses FEA simulation to observe the GBP behavior under a hydraulic crane to facilitate more informed decision making.

5. Future research directions

The significance of a critical lift always raises concerns among practitioners. The calculation of GBP is vital so that it can be compared with the soil bearing capacity. If the GBP is greater than the soil bearing capacity, crane mats made of wood or steel are used to distribute the load and decrease the magnitude of the GBP, lowering it to within the limits of the soil bearing capacity. With the increased use of heavy cranes due to modularization, ignoring the GBP at the edges of the crane mat and only taking the average over the crane mat surface area can lead to poor ground preparation for crane operation on a construction site. It is important to calculate an accurate GBP distribution under hydraulic crane mats to determine whether the soil can bear the load or not, and further to select the appropriate crane mat for the crane task. Crane failure due to crane tipping is consistently a grave concern for the safety of workers working around cranes. In the context of lean construction methodology as applied to modular construction, if reducing the waste by selecting the size of the crane mat based on the traditional GBP calculations, the likelihood of ground failure would increase. Moreover, mobile crane utilization optimization should incorporate the proposed method (i.e., the proposed set of equations for GBP calculations) to determine the GBP under hydraulic crane outrigger mats.

In addition, the proposed method should be implemented and tested in other theoretical case studies where the load is maximum and the crane mats opposite to the payload show zero GBP under the crane mats. This phenomenon develops a GBP diagram that is triangular in nature, instead of trapezoidal. These are the scenarios in which the crane is very close to tipping and one or more of the crane mats are taking no load [11,12]. The results presented herein indicates it is important to investigate these scenarios where the GBP is distributed over three or fewer than three outrigger crane mats.

In addition, it is also important to calculate the GBP under crawler crane tracks. In the case of GBP calculations under crawler crane tracks, it is assumed that pressure is uniform along the width of the track [11–13,15,16]. But considering the findings of the present study, the author believes that the GBP under crawler crane track along the track width is not uniform in nature. As the application and usage of crawler cranes has increased in the last decade due to modular construction, it is important to determine these variations under crawler crane tracks in order to select the right crane mat for the job.

In conclusion, to facilitate the work undertaken by practitioners in this domain and also to align with Construction 4.0 practices, it be worthwhile to develop a computer application for such new calculation methods for general and practical use.

References

[1] Osunsanmi, T. O., Aigbavboa, C., & Oke, A. (2018). Construction 4.0: The Future of the Construction Industry in South Africa. World Academy of Science, Engineering and Technology, International Journal of Civil, Environmental, Structural, Construction and Architectural Engineering, **12** (**3**), 206–212

[2] Oesterreich, T. D., & Teuteberg, F. (2016). Understanding the implications of digitisation and automation in the context of Industry 4.0: A triangulation approach and elements of a research agenda for the construction industry. Computers in Industry, **83** (**10**), 121–139. https://doi.org/https://doi.org/10.1016/j.compind.2016.09.006

[3] Jostein, P. (2009). Defining lean production: some conceptual and practical issues. The TQM Journal, **21** (**2**), 127–142. https://doi.org/10.1108/17542730910938137.

[4] Sawhney, A., Riley, M., & Irizarry, J. (2020). Construction 4.0: An Innovation Platform for the Built Environment. Routledge, London [UK]. https://doi.org/10.1201/9780429398100.

[5] Hamid, A., Rahim, A., Azhari, R., Zakaria, R., Aminudin, E., Putra Jaya, R., Nagarajan, L., Yahya, K., Haron, Z., & Yunus, R. (2019). Causes of crane accidents at construction sites in Malaysia. IOP Conference Series: Earth and Environmental Science, **220** (**1**). 1–10 https://doi.org/10.1088/1755-1315/220/1/012028

[6] Aikhuele, D. (2019). Evaluation of the root cause of failure in a crawler crane machine using hybrid MCDM model. Transactions of the Royal Institution of Naval Architects Part A: International Journal of Maritime Engineering, **161**, 219–228. https://doi.org/10.3940/rina.ijme.2019.a3.523.

[7] Cho, C.-S., Boafo, F., Byon, Y.-J., & Kim, H. (2017). Impact analysis of the new OSHA cranes and derricks regulations on crane operation safety. KSCE Journal of Civil Engineering, **21** (**1**), 54–66. https://doi.org/10.1007/s12205-016-0468-7

[8] Dhalmahapatra, K., Singh, K., Jain, Y., & Maiti, J. (2018). Exploring Causes of Crane Accidents from Incident Reports Using Decision Tree. In S. C. Satapathy & A. Joshi (Eds.), Information and Communication Technology for Intelligent Systems (pp. 175–183). Springer Singapore.

[9] Milazzo, M. F., Ancione, G., Spasojević-Brkić, V., & Valis, D. (2016). Investigation of crane operation safety by analysing main accident causes. ESREL 2016, Glasgow, Scotland. https://doi.org/10.1201/9781315374987-14.

[10] Raviv, G., & Shapita, A. (2017). Systematic approach to crane-related near-miss analysis. The International Journal of Construction Management, **8**(**4**), 310–320.

[11] Shapiro, J., & Shapiro, L. (2010). Cranes and Derricks, (4th ed.). McGraw-Hill Professional.

[12] Becker, R. (2001). The Great Book of Mobile and Crawler Cranes: Handbook of mobile and crawler crane technology (Issue v. 1). René Hellmich.

[13] Hasan, S., Al-Hussein, M., Hermann, U., & Safouhi, H. (2010). Interactive and Dynamic Integrated Module for Mobile Cranes Supporting System Design. Journal of Construction Engineering and Management, **136** (**2**). https://doi.org/10.1061/(ASCE)CO.1943-7862.0000121.

[14] Ali, G. M., Al-Hussein, M., Bouferguene, A., & Kosa, J. (2019). Competitive finite element analysis (ANSYS) for the use of ice & frozen silt as a supporting structural material, an alternative to the traditional crawler crane mat material (S355, G40.21 & Coastal Douglas-fir). CSCE Annual Conference Growing with Youth – Croître Avec Les Jeunes, (pp. 1-10).

[15] Ali, G. M., Al-Hussein, M., Bouferguene, A., & Kosa, J. (2018). Use of ANSYS for calculating ground bearing pressure under crawler crane tracks and pad load under the outriggers of hydraulic cranes. Proceedings, Canadian Society for Civil Engineering Annual Conference, (pp. 1-10).

[16] Di, W., Yuanshan, L., Xin, W., Xiukun, W., & Shunde, G. (2011). Algorithm of Crane Selection for Heavy Lifts. Journal of Computing in Civil Engineering, **25** (**1**), 57–65. https://doi.org/10.1061/(ASCE)CP.1943-5487.0000065.

[17] Hibbeler, R. C. (2011). Mechanics of Materials (8th ed.). Pearson Prentice Hall.

[18] Hally, D. (1986). Calculation of the moments of polygons. Applied Mathematics Notes.

[19] Manitowoc. (2020). GMK7550. [Online] Available: https://www.manitowoccranes.com/en/cranes/grove/grove-products/all-terrain/GMK7550 [Accessed June 19, 2020].

[20] Craneaccidents.com. (2020). Crane Accidents. [Online] Available: https://www.craneaccidents.com/archive/. [Accessed June 20, 2020]

[21] Beavers, J., R. Moore, J., Rinehart, R., & R. Schriver, W. (2006). Crane-Related Fatalities in the Construction Industry. Journal of Construction Engineering and Management-ASCE, **132**(**9**), 901–910. https://doi.org/10.1061/(ASCE)0733-9364(2006)132:9(901)